



Calhoun: The NPS Institutional Archive

Faculty and Researcher Publications

Faculty and Researcher Publications Collection

2010-05

A mobile phased array Doppler radar for the study of severe convective storms

Bluestein, Howard B.

American Meteorology Society

Bulletin of the American Meteorological Society, v. 91, no.5, May 2010, p. 570-586

<http://hdl.handle.net/10945/48186>



Calhoun is a project of the Dudley Knox Library at NPS, furthering the precepts and goals of open government and government transparency. All information contained herein has been approved for release by the NPS Public Affairs Officer.

Dudley Knox Library / Naval Postgraduate School
411 Dyer Road / 1 University Circle
Monterey, California USA 93943

<http://www.nps.edu/library>



Calhoun: The NPS Institutional Archive

Faculty and Researcher Publications

Faculty and Researcher Publications Collection

2010-05

A mobile phased array Doppler radar for the study of severe convective storms

Bluestein, Howard B.

American Meteorology Society

Bulletin of the American Meteorological Society, v. 91, no.5, May 2010, p. 570-586
<http://hdl.handle.net/10945/48186>






Calhoun is a project of the Dudley Knox Library at NPS, furthering the precepts and goals of open government and government transparency. All information contained herein has been approved for release by the NPS Public Affairs Officer.

Dudley Knox Library / Naval Postgraduate School
411 Dyer Road / 1 University Circle
Monterey, California USA 93943

<http://www.nps.edu/library>

[< Back to results](#)[More like this >](#)

A MOBILE, PHASED-ARRAY DOPPLER RADAR FOR THE STUDY OF SEVERE CONVECTIVE STORMS

Bluestein, Howard B ; French, Michael N; PorStefanija, Ivan; Bluth, Robert T ; Knorr, Jeffrey B . **Bulletin of the American Meteorological Society** 91.5 (May 2010): 579.

[Full text](#)[Abstract/Details](#)[References 35](#)

Abstract [Translate](#)

(1999) found after inspecting Weather Surveillance Radar-1988 Doppler (WSR-88D) volume scans that some tornadic vortex signatures descend, whereas others appear in a column simultaneously. Since it takes ~4-5 min to complete a volume scan (Crum and Alberty 1993), the latter finding might not hold for shorter time scales: A midlevel (~5 km AGL) vortex advected downward by a downdraft of -20 m s^{-1} for 4 min will descend ~5 km (i.e., down to the ground); with observations on a 4-5-min time scale, the descent would appear to be simultaneous.

Full Text [Translate](#)

Headnote

In a recent field experiment a truck-based, rapid * scan, agile-beam Doppler radar probed severe convective storms and tornadoes on very short time scales, at relatively close range.

Many severe convective storms and tornadoes evolve on time scales shorter than, that resolved by most mechanically scanning radar systems. For example, the advective time scale of a tornado is $\sim 2\pi r / V$, where r is the core radius of the tornado and V is the wind velocity scale. For a tornado having a core radius of 100 m (e.g., Wurman and Gill 2000; Bluestein et al. 2003; Tanamachi et al. 2007) and wind speeds of $\sim 60 \text{ m s}^{-1}$, the advective time scale is only 10 s. Bluestein et al. (2003; their Figs. 10 and U) showed how even when the reflectivity and Doppler wind field in a tornado at low levels is viewed every ~15 s, not all the evolution is captured.

In a supercell having updrafts of -50 m s^{-1} (e.g., Weisman and Klemp 1984, their Fig. 5; Bluestein et al. 1988, their Fig. 15), vortices, cloud particles, small hydrometeors, etc., can be advected upward ~5 km, almost half the depth of the parent storm in just ~100 s (a few min). Trapp et al. (1999) found after inspecting Weather Surveillance Radar-1988 Doppler (WSR-88D) volume scans that some tornadic vortex signatures descend, whereas others appear in a column simultaneously. Since it takes ~4-5 min to complete a volume scan (Crum and Alberty 1993), the latter finding might not hold for shorter time scales: A midlevel (~5 km AGL) vortex advected downward by a downdraft of -20 m s^{-1} for 4 min will descend ~5 km (i.e., down to the ground); with observations on a 4-5-min time

scale, the descent would appear to be simultaneous. Rasmussen et al. (2006) have suggested that descending reflectivity cores (DRCs) may play a role in tornadogenesis. DRCs in strong downdrafts may also require rapid sampling to be resolved adequately.

A phased-array (electronically scanning, "agilebeam"), fixed-site, S-band Doppler radar [the National Weather Radar Testbed Phased Array Radar (NWRT PAR)] has been used to obtain rapid-scan observations (volumetric update time ~30 s to 1 min) of a microburst, supercells, and a tornadic supercell (Zrnic et al. 2007; Heinselman et al. 2008). Having a halfpower beamwidth of ~1.5°-2.0°, the PAR's azimuthal spatial resolution is ~150 m or better only for storms within ~5-km range; such resolution is needed to resolve features as small as ~1.5 km in scale (i.e., including mesocyclones and other storm-scale features).

To increase the likelihood that any radar is located near enough to convective storms that the spatial resolution is ~150 m or better, it is useful that the radar be mobile. Most existing ground-based mobile radar antennas scan mechanically and their volumetric (from near the ground up to at least halfway to the tropopause) update time is at least 1-2 min (e.g., Biggerstaff et al. 2005; Bluestein 2009). In order to keep the antenna small enough so that it can be mounted on a truck, yet also not be so susceptible to attenuation that scatterers at ranges up to ~30-60 km cannot be detected, most mobile radars for storm-scale applications operate at X-band or C-band.

Two mobile radars currently exist that can collect "rapid-scan" data at X-band. The Rapid Doppler on Wheels (DOW; www.cswr.org/docs/radarconf-rapid-2001-0327.pdf) at the Center for Severe Weather Research (CSWR) uses a multiple-frequency technique to scan electronically in elevation while scanning mechanically in azimuth. The purpose of this paper is to describe another mobile X-band radar that leverages existing military phased-array technology (Pazmany 2007) and to identify possible scientific issues to be addressed in further, more detailed studies. The radar has several key features that make it well suited for severe weather research, including pulse-to-pulse elevation plane beam steering for rapid volume imaging and electronic backscanning in azimuth to avoid beam smearing.

CHARACTERISTICS OF THE MWR-05XP. The Meteorological Weather Radar 2005 X-band Phased Array (MWR-05XP) is an Army tactical radar modified by ProSensing, Inc., for meteorological and other distributed target applications (Sandifer 2005). Mounted on a heavy-duty truck (Fig. 1a), the MWR-05XP can be deployed in ~5 min. A summary of the characteristics of the radar system is found in Table 1.

Scanning strategies. The radar's antenna is a hybrid, with pulse-to-pulse electronic elevation scanning, limited electronic azimuth scanning, and rapid mechanical azimuth scanning. Electronic scanning in elevation angle is accomplished by changing the phase delay among the antenna elements using phase shifters; electronic scanning in azimuth (over a limited sector) is accomplished by changing the frequency ("frequency hopping," which is made possible because the radar has "frequency agility") of beams coming out of a slotted waveguide such that the phases are changed as the frequency is changed (Skolnik 1990). A DC stepped motor is used to scan in azimuth at a variable rate with a maximum speed of 180° s⁻¹. This revolution rate is much higher than that of typical ground-based mobile Doppler radars (~6°-12° s⁻¹). Conventional radars scanning at such high rates cannot gather enough independent samples to produce meaningful estimates of Doppler velocity. The MWR-05XP employs frequency hopping also to generate more independent samples; the hopping occurs every other radar pulse. This hopping allows pulse pairs to be formed at a common frequency for Doppler velocity estimation.

Frequency shifting by at least l/t , where t is the pulse length, results in a statistically independent sample of the radar echo from a distributed target. The antenna beam is steered electronically in the opposite direction of the mechanical scan over a narrow sector. This back scanning allows the beam to dwell at a nearly fixed azimuth angle during the time required to gather independent samples. Thus, frequency hopping is employed both to eliminate azimuthal beam smearing and to increase the number of independent samples.

Two modes of data collection are employed. The first is a stepped frequency spiral (STF-SP) volumetric scan sequence covering a full 360° in azimuth over overlapping elevation angles; the scan increment in elevation angle is set to an angle less than the elevation beamwidth of the antenna. This mode, which is similar to that used by the WSR-88D but is 10 times faster, is best suited for surveillance or when coverage of more than one convective storm or a broad area of precipitation (e.g., a mesoscale convective system) is required. The elevation angle is changed after each full 360° in azimuth has been scanned. It takes ~ 25 s to complete a full volume scan from 0° to 20° in elevation angle. Volume scans up to higher elevation require proportionally longer times. For simple surveillance, the highest elevation angle scanned can be reduced to 10° , so that the volumetric update time is only ~ 10 - 15 s. Beam smearing is eliminated through electronic back scanning.

The second mode of data collection is a stepped frequency elevation (STF-E) volumetric sector-scan sequence. In the STF-E mode, the antenna's elevation angle is electronically changed after transmitting a pair of radar pulses to step rapidly through the desired elevation angle range. Ten sequential elevation-angle scans are collected as the antenna mechanically scans in azimuth before returning to the initial elevation angle (~ 10 ms return time). The 10 consecutive elevation scans are then averaged to obtain statistically significant estimates of reflectivity and velocity. To minimize beam smearing in azimuth during the 2008 season, when frequency agility for backscanning was not implemented, the antenna rotation rate was slowed down to rotate ~ 6 during the time it took to collect 10 elevation-angle scans. In this case, the total scanning time was ~ 13 s to sample a sector covering 90° in azimuth and 20° in elevation angle. The scanning mode unique to the 2008 field experiment is called sector elevation (SE). In the spring of 2009, frequency hopping, providing at least 10 (and up to 32) independent samples per averaged beam, was added to eliminate the effects of beam smearing and the antenna rotation rate was increased. With frequency hopping implemented (STF-SE), a higher antenna rotation rate was possible because independent samples were obtained at a higher rate, reducing the volume sampling time by a factor of 2; by comparison, a conventional radar without frequency hopping would have to dwell at the same position in space 10 times the weather target decorrelation time to obtain the same number (10) of independent samples. (The update times shown in Table 1 for 2009 in STF-SE mode account for the slowing down of the antenna before it reverses direction.)

Spatio/ resolution. Since the beamwidth of the antenna is approximately twice that of most mobile X-band Doppler radars, the MWR-05XP is most useful for storm-scale observations, not for probing tornadoes with high spatial resolution. At a range of ~ 10 - 20 km, the azimuthal resolution is ~ 300 - 600 m, which is good enough to resolve (it is assumed that the spatial resolution must be about one tenth or less of the scale of the feature being sampled) mesocyclones and other features broader than ~ 2.5 - 5 km, but not tornadoes, most of which tend to have core radii of ~ 100 m. Beyond 20-km range, small mesocyclones (~ 2.5 km in scale) may not be adequately sampled in the cross-beam direction; however, in the radial direction the resolution (150 m) is still adequate to detect the divergent/convergent aspect of mesocyclones (Brown and Wood 1991). Only if the radar is positioned within 5 km

of the tornado and if the tornado is broad (-2 km or more across) is there any possibility of resolving its airflow. (However, in order to detect a tornado, but not necessarily to resolve the airflow well, the spatial resolution may be only about one quarter to one fifth the scale; thus, at 5 km the radar can detect a tornado -1 km across.)

Doppler velocity estimation. Doppler velocity is estimated using standard pulse-pair processing techniques (e.g., Sirmans and Doviak 1973). Sources of error include ground clutter contamination, which can bias velocities toward zero, or bimodal spectra, which can also bias velocities toward zero if the radar beam encompasses all of a tornado vortex. The variance of the velocity estimate decreases as the number of independent samples and signal-to-noise ratio increase. For a pulse-repetition frequency (PRF) that corresponds to a maximum unambiguous range of 60 km [2.5 kHz; 400- μ s pulse repetition time (PRT)], an integration time of 9 ms, and 10 samples, the estimated velocity error is ± 2.4 , ± 0.6 , ± 0.2 , and ± 0.06 m s⁻¹ for signal-to-noise ratios of 0, 10, 20, and 30 dB, respectively.

Velocity spectra may be computed using the fast Fourier transform (FFT) algorithm, but doing so would increase the total scan time by at least an order of magnitude. The calculation of spectra might be useful when the radar beam encompasses all of a tornado, but the rapid-scan capabilities of the radar would then be defeated. Ground clutter removal by filtering out Doppler velocities of near-zero velocity also requires use of the FFT and so also can increase the scan time substantially. In addition, it cannot be used together with frequency agility. For these reasons, ground clutter removal algorithms were not implemented. It would be possible to turn on a ground clutter algorithm only for the lowest elevation scan, thus increasing the volumetric scan time by not as much as it would be if it were turned on for all elevation angles. To date, however, this has not been done.

The typical PRT of 400 μ s yields a maximum unambiguous velocity of 20 m s⁻¹ and an unambiguous range of 60 km. Aliasing can be corrected relatively easily manually or with simple algorithms at low altitudes, but is difficult, if not impossible, to do aloft when wind speeds are very high and there are sharp spatial gradients in velocity (e.g. when there is a strong mesocyclone or strong divergence above an updraft). Use of staggered PRF can produce higher unambiguous velocity, but doing so doubles the scan time. Beginning in 2010, a new data collection technique will be employed using two different PRFs on alternate sweeps of the desired volume sector. This technique does not result in an increase in volume scan time. Thus, if the time scale of evolution is relatively slow compared with the total volume scan time, it will be possible to use temporal continuity in a qualitative sense as a means of correcting for aliasing.

Navigation parameters. The orientation and location of the radar truck are determined from a dual-antenna GPS system. While efforts are made to level the radar system, it is not always possible to find terrain with a shallow enough slope to level the radar system perfectly. The attitude of the radar truck in a ground-relative reference frame is determined, after best attempts at leveling the truck, from a digital inclinometer; the pitch, roll, and heading angles are known to within 0.1°.

FIELD TESTING OF THE MWR-05XP. EXAMPLES OF DATA COLLECTED. The MWR-05XP was field tested in the U.S. Great Plains (Fig. 1b) for about a month in the spring of 2007 (Table 2) and 2008 (Table 3). Based at the University of Oklahoma, field operations were conducted mainly in parts of Oklahoma, Texas, and Kansas, but also on rare occasions, especially near the end of the field programs, in Nebraska, when the likelihood of severe weather typically migrates northward with the upperlevel westerlies. Field operations were conducted in a manner similar to those of earlier severe-storm intercept projects (e.g., Bluestein 1999), but most of the information received in

the field was from weather data viewed over the internet on a laptop computer via a cell-phone internet connection, rather than from a nowcaster back in Norman. Since software development was ongoing in 2007 and 2008, only stepped frequency spiral volume scans were available in 2007; stepped frequency elevation volume scans became available after the first deployment in 2008.

On some occasions radar data were also collected in conjunction with X- and W-band radars from the University of Massachusetts (UMass) (e.g., Bluestein et al. 2007a). However, since the MWR-05XP had much longer setup and tear-down times, it was necessary on most occasions to deploy the radar truck far in advance of an oncoming storm and wait for the storm to approach the radar and then to cease data collection well in advance of the storm's arrival at the deployment site. It was also more difficult to find a deployment site, owing to the truck's larger size. As a result, data collection at the same site as one of the UMass radars happened relatively rarely and in fact sometimes the radars sampled different storms.

To demonstrate that the MWR-05XP collects qualitatively reasonable data, a number of selected cases are briefly presented for nontornadic and tornadic supercells and for quasilinear mesoscale convective systems (MCSs). In one case, the MWR-05XP data will be compared with data from another co-located X-band radar and from a nearby WSR-88D radar. For some cases, special features uniquely suited for study by rapid-scan radars will be pointed out. In addition, some important scientific problems that maybe addressed using rapid-scan data will be noted.

In most of the cases discussed below, data for which the radar reflectivity factor was less than 0 dBZ were discarded and velocity data were de-aliased using both objective and manual methods.

Supercells. Since supercells spawn the largest, most intense tornadoes, it is important to be able to sample the wind and reflectivity fields in them. Examples of classic high-precipitation (HP) supercells are shown, as well as a low-precipitation (LP) one (e.g., Rasmussen and Straka 1998), which illustrate a number of characteristic structures. These examples are not intended to be exhaustive and space limitations preclude showing full three-dimensional depictions for each storm, let alone their temporal evolution. Detailed scientific discussions are beyond the scope of this discussion.

23 MAY 2007: CLASSIC AND HP supercells. Two classic supercells depicted at low levels at ~20-km range display a characteristic concave curvature in reflectivity on their right rear flanks (Fig. 2a). These were the first supercells observed by the MWR-05XP. The newer supercell to the west had a weak cyclonic vortex signature (Fig. 2b) coincident with a hook echo (Fig. 2a). A wall cloud and typical cloud-base structure were observed in this supercell (Fig. 3a), but no tornadoes were noted.

Towards evening, an HP supercell (Fig. 3b) was probed by the MWR-05XP. This storm had a typical bulging rear-flank gust front composed of heavy precipitation and a cyclonic vortex signature near the back edge of an echo-weak notch (Fig. 4a). The leading edge of the rear-flank gust front, probably marking the leading edge of the rear-flank downdraft (RFD), is evident as a curved gradient in Doppler velocity emanating from the cyclonic vortex signature (green to white to yellow arc).

27 May 2008: HP SUPERCELL. A classic supercell that remained stationary, but then collapsed as precipitation fell out and assumed the characteristics of an HP supercell, with an arcus cloud along the edge of the RFD (Fig. 5a), was sampled both before (Fig. 4b) and after it collapsed (not shown). While the hook echo associated with it was relatively far away (-40-45 km in range), it had a region of cyclonic shear that was coincident with the tip of the hook and a weak-echo eye at low levels (Fig. 4b).

5 June 2008: HP SUPERCELL. An HP supercell that had collapsed and had an extensive weak-echo notch did not have any vortex signatures at the time of data collection (Fig. 4c). It was unusual to find that the echo associated with the RFD was more extensive than the echo associated with the forward-flank downdraft (FFD). The RFD echo had wrapped cyclonically around the point of intersection of the FFD echo and RFD echo so that it was located on the southeast of the FFD echo, a configuration that is unusual. This storm produced tennis-ball size hail, which was documented by the first author, who was in the UMass W-band radar at the time the MWR-05XP was collecting data (Fig. 5b). Scientific questions that should be addressed are why the RFD echo was so extensive, why the hail was so large, and why no tornadoes were spawned, all of which were likely related. For this case, however, not enough volume scans are available to address these questions because the radar had to move to avoid getting hit by the large hail.

31 May 2007: HP SUPERCELL. An HP supercell that ultimately produced a weak tornado, but was not probed at the time of tornadogenesis because the radar truck was in transit, was remarkable in the clarity of its structure, even though it was at a relatively long range (-40-45 km). This supercell had a well-defined hook echo at low levels accompanied by a broad cyclonic vortex signature (Fig. 6a). Of all the supercells sampled by the MWR-05XP, this one displayed the most prominent radar signatures aloft: A U-shaped weak echo region (WER) almost completely surrounded a region of high reflectivity (Fig. 6b) above the low-level hook echo. This WER, which was co-located with a very broad cyclonic vortex signature, was likely near the main updraft of the supercell. At very high levels, some of the U-shaped WER still appeared (Fig. 6c). The physical meaning of this U-shaped WER is worthy of further analysis.

1 JUNE 2007: HP SUPERCELL. An HP supercell that developed a pronounced cyclonic vortex signature well behind the rear-flank gust front at low levels (Fig. 7) was located at the southern edge of a broad mass of precipitation. The apparent cyclone was not visible since it was hidden behind an area of extensive precipitation (Fig. 8). The development of this vortex is worthy of detailed analysis, especially since it did not appear to develop along the ends of a convective line as many vortices do in bow echoes (Weisman and Davis 1998).

22 MAY 2008: LP SUPERCELL. The only LP supercell sampled by the MWR-05XP was at very close range (the closest range to the radar echo was only 5 km; see Fig. 9). Unlike the HP supercells, for which an extensive radar echo was associated with the rearflank gust front, this LP supercell's rear-flank gust front was marked by a relatively thin line of radar echo. An appendage was located where the hook echo would ordinarily be and was connected to the main mass of radar echo to the north.

A hook echo with an anticyclonic vortex signature, however, was located 7.5 km to the southeast. About 26 min earlier, the region under cloud base was translucent, while some precipitation (opaque region) was evident on the northern end of the cloud base, extending to the north a bit, but then becoming more translucent to the northeast (Fig. 10). While no cyclonic vortex signature was evident in association with the appendage, there was a maximum

of outbound flow, but no detectable scatterers where an inbound part of a rotational couplet would have been. It is not known if there was no cyclonic vortex near the appendage, or there in fact was one but it was not detectable, owing to a paucity of scatterers. Anticyclonic vortices or even anticyclonic tornadoes have been documented along the end of rear-flank gust fronts (Brown and Knupp 1980; Fujita 1981; Markowski 2002; Bluestein et al. 2007b). Weisman and Davis (1998) have suggested that tilting of baroclinically generated horizontal vorticity along the leading edge of a cold pool or existing low-level environmental shear could lead to counter-rotating vortices along the ends of the line of convection when an updraft is present above cloud base. Markowski et al. (2008) presented observational evidence that this mechanism is responsible for producing cyclonic-anticyclonic couplets along the rearflank gust front in supercells. Since volumetric data are available at 13-s intervals and the anticyclone was so near (-6.5 km in range) to the radar that the spatial resolution is only 150 m (range) x 200 m (azimuth) x 225 m (elevation), this case merits further analysis with the aim of elucidating the genesis mechanism of the anticyclonic vortex.

Tornadic supercells. Because tornadoes have short time scales, rapid-scan radars are well suited for probing them with the aim of understanding tornadogenesis. However, because their spatial dimensions are so small, it is necessary that radars get as close to them as possible. The MWR-05XP collected data in a number of tornadoes and captured tornadogenesis in at least one instance. Issues such as the effects of attenuation and the maximum range at which tornadogenesis can be observed with the MWR-OXP are now addressed.

1 MAY 2008: ISOLATED SUPERCELL. The MWR-05XP first probed a tornado at a range of -20-25 km in northeast Oklahoma. A well-defined hook echo and evidence of a trailing rear-flank gust front and a cyclonic vortex signature coincident with the tip of the hook were seen (Fig. 11a) at the time of one of the tornadoes observed in this storm (Fig. 12). The wind speeds associated with the vortex signature, however, were not very strong (maximum outbound velocities of -28 m s⁻¹) at a 2° elevation angle (-800 m AGL). The parent supercell (cell B) moved rapidly away from the radar (Fig. 11b) but still maintained a well-defined hook echo as tornadoes continued to be reported after dark. The volumetric update time for this dataset was -65 s because it was in STF-SP mode and it was its first day of operation in 2008, when software were still being developed and applied for the first time. While this dataset is not optimal for studying tornadogenesis, it was possible to document simultaneously a nearby nontornadic supercell (cell A) also, and especially its decay as it passed near the radar. Bluestein (2008) has discussed how some supercells decay via a "downscale transition," and cell A on radar appears to have decayed via this process as it became narrower with time (not shown).

10 MAY 2008: ISOLATED SUPERCELL. Tornadogenesis occurred during data collection in a supercell that produced a waterspout over a lake in eastern Oklahoma, at a range of just over 20 km. This volumetric dataset, while acquired with an update time of -13 s, was obtained under suboptimal circumstances because the MWR-05XP was located just downstream from the parent supercell. Cloud features were not visible through intervening precipitation and attenuation was significant. The evolution of the parent vortex is best viewed at -3 km AGL in the storm (8.9° elevation angle) (Fig. 13). A cyclonic vortex signature appeared in a hook echo and developed on very short time scales (cf. Figs. 13a-c). It is not known if the evolution of the vortex was really fast or if it became visible on short time scales, owing to an early paucity of scatterers. In the latter case, the time scale of evolution of reflectivity was short. In this case, however, there is evidence that attenuation may have led to the extinction of the radar signal and the rapid change in appearance may have been a result of storm motion and a change in pathintegrated attenuation: At 8.9° elevation angle the path of the radar beam was through less than 5 km of

relatively high reflectivity (Fig. 13h), whereas at 1° elevation angle, the path of the radar beam was through -7.5 km of high reflectivity and a few even more intense cores (Fig. 13g). Thus, the hook echo (and concomitant tornado) was not detected at low elevation angles. It is concluded that the M WR- 05XP should not be deployed just upstream from supercells if at all possible to minimize the possibility of extinction of the radar signal at the range of possible tornadoes.

At 18.4° elevation angle (-6.7 km AGL) a weak echo notch (not shown) was coincident with the hook and cyclonic vortex signature below at 3 km AGL. This notch narrowed steadily, from -5 km wide at 2222:25 UTC (all times given in UTC; CDT is 6 h earlier) to just ~2 km, 1 min later, at 2223:25 UTC, while the tornado was forming. Such a narrowing, which may have been undetected by conventional, more slowly scanning radars, maybe related to the collapse of the storm's updraft, or the narrowing of the storm's updraft.

23 May 2008: Supercells. A number of tornadic supercells were probed on this day in Kansas. None of the supercells were completely isolated, as there were nearby neighboring or connected storms. In the best dataset collected by the MWR-05XP, volumetric data to 20° elevation angle (-6.5 km AGL) were recorded for 13-s updates, for -50 min, covering a time span from -15 min prior to tornadogenesis until well after tornado dissipation, at a range varying from -16 km during tornadogenesis to -20 km during dissipation. The tornado probed is known as the "Hog Back tornado." Images of Doppler velocity for 1° elevation angle (-300 m AGL) at 13-s intervals (Fig. 14) resolve an increase in inbound wind speeds steadily from -20 m s⁻¹ at 0201:58 UTC to 30 m s⁻¹ at 0203:36 UTC and a leveling off thereafter at -36 m s⁻¹. Outbound velocities, however, increased from -15 m s⁻¹ at 0201:58 UTC to 72 m s⁻¹, when the shear associated with the cyclonic vortex signature due to the tornado was most intense. At this time, and others, wind speeds of -0-9 m s⁻¹ were noted at the center of the vortex signature, which is consistent with the averaging of a tornado vortex spectrum having opposing maxima closer than 1 km from each other and a small component of translation away from the radar, as was noted. The actual tornado was probably situated on the side of its parent cyclone because the vortex (dipole in isodops) signature was not symmetrical about -0-9 m s⁻¹ but was rather displaced significantly toward the outbound side (e.g., at 0205:58 UTC the maximum outbound velocities were -72 m s⁻¹ while the maximum inbound velocities were only -27 m s⁻¹; Fig. 14c). The complete analysis of this dataset at all elevation angles is forthcoming and the usefulness of such a dataset in elucidating tornadogenesis and tornado dissipation will be evaluated.

Another tornado captured in the same dataset, but -20 km to the west-northwest rather than to the northwest of the radar (like the Hog Back tornado), the "Ellis tornado 1" was already mature at the outset of data collection at 0148:57 UTC (Fig. 15a). The cyclonic vortex signature at this time was characterized by a couplet of Doppler velocities of ±35-40 m s⁻¹. The dataset does, however, capture the complete life cycle of a nearby anticyclonic vortex that intensified, reaching a maximum intensity at 0152:16 UTC (Fig. 15b) (having maximum outbound velocities of -35 m s⁻¹). While no tornado was reported in association with this vortex, note that it was dark at the time, there may have been no structures to damage along its path, or it might have too weak to inflict any damage. The vortex began -2.5 km east southeast of its cyclonic neighbor (Fig. 15a) and rotated cyclonically about its cyclonic neighbor, ending up to its northeast by -6 km (Fig. 15c). This anticyclonic vortex may have been similar to the one described earlier (Fig. 9b) and by the ones documented by Brown and Knupp (1980), Fujita (1981), and Bluestein et al. (2007b). Detailed analysis of the evolution of this anticyclonic vortex is

therefore warranted so that its formation and dissipation might be explained. This case and that of the much weaker anticyclonic vortex observed on 22 May 2008 beg the questions: Why do anticyclonic vortices form only on certain instances, and why do they only rarely develop into anticyclonic tornadoes?

Quasilinear mesoscale convective systems. As producers of severe weather and occasionally tornadoes, quasilinear mesoscale convective systems are worthy of study. A representative sample of several quasilinear MCSs is highlighted.

21 MAY 2007: SEVERE SQUALL LINE. On this date an intercomparison between data collected by the MWR-05XP, the UMass X-Pol (Kramar et al. 2005), and a WSR-88D was conducted in the northern Texas Panhandle as a squall line approached (Fig. 16). This squall line produced hail to 3.8 cm in diameter and wind gusts to 34 m s^{-1} . The shape of the radar reflectivity field associated with the squall line at low elevation angle as viewed by the MWR-05XP (Fig. 17a) was similar to that as viewed by the UMass X-Pol (Fig. 17c) and the WSR-88D (Fig. 17e); a concavity in the leading edge and a more linear section to its northeast are both resolved. The stratiform region to the northwest of the leading convective line was - as would be expected by an X-band radar - much more attenuated than it was by the S-band WSR-88D. Both the MWR-05XP and the UMass X-Pol exhibited notches of weaker echo on the backside that were likely caused by attenuation to extinction. Both the MWR-05XP and the UMass X-Pol resolved a maximum in inbound velocities -25 m s^{-1} near one portion of the leading convective line (Figs. 17b,d); a second one was resolved by the MWR-05XP but not by the UMass X-Pol. In general, the attenuation experienced by the MWR-05XP seemed to be less than that experienced by the UMass X-Pol for reasons that are unknown.

29 May 2007: Severe squall line. A classic squall-line segment, having a leading low-elevation fine line (Fig. 18a) marking the wind shift (Fig. 18b) of its gust front, passed by close to the MWR-05XP. It is noteworthy that the MWR-05XP was able to resolve the fine line and its associated wind field, which was at very close range ($\sim 6 \text{ km}$). This squall line produced hail up to 2.5 cm in diameter.

8 MAY 2007: MESOSCALE CONVECTIVE SYSTEM WITH EMBEDDED MESOCYCLONE. On this day, the first for which MWR-05XP data were collected in a convective storm of any kind, a rare tornadic storm in a mesoscale convective system was sampled at very long range ($\sim 60 \text{ km}$). At this range the azimuthal resolution of the radar antenna is $\sim 1.9 \text{ km}$. The volumetric update time was $\sim 25 \text{ s}$ and data were collected up to a 13.2° elevation angle, which at the range of the storm was just above 13 km AGL . The radar serendipitously probed a cell that formed ahead of the leading convective line in the northeastern quadrant of an asymmetric bow-echo MCS (Houze et al. 1990; Weisman 1993) (Fig. 19), which had just produced a small tornado. The MCS had a mesoscale convective vortex (MCV), but the storm that had produced the tornado was not coincident with the MCV (Fig. 19d). Hail up to 2.5 cm in diameter was also reported.

Despite having very coarse spatial resolution, the MWR-05XP was able to resolve a cyclonic vortex signature (Fig. 19b) that was also resolved by a WSR-88D (Fig. 19d). The shape of the radar echo seen by the MWR-05XP was similar to that seen by the WSR-88D (Figs. 19a,c): The vortex signature was very near, but not coincident with a weak echo hole; the parent storm exhibited a weak echo region (WER) to the south of the weak echo hole. The overall shape of the radar echo, however, was unlike that of a classic supercell. Tornadoes and vortices within

quasilinear MCSs have been studied by Trapp et al. (2005). A detailed analysis of this case, notwithstanding the coarse spatial resolution, might yield additional insight into the structure and dynamics of tornado-producing cells in MCSs, as a result of the relatively high temporal resolution of the MWR-05XP data.

SUMMARY AND CONCLUSIONS. Field operations using the MWR-05XP have proven successful in collecting "rapid-scan," storm-scale, Doppler data in severe convective storms, particularly in tornadic supercells when features evolve very quickly as a result of high wind speeds and strong updrafts and downdrafts.

Efforts will be undertaken to determine how useful rapid-scan, storm-scale observations actually are. In this paper it has been shown that the reflectivity and Doppler velocity fields in convective storms probed by the MWR-05XP either compare well qualitatively with data collected by other radars or represent idealized phenomena well.

However, it has not been demonstrated yet whether having rapid-scan observations can actually improve our physical understanding or our ability to make more accurate numerical forecasts.

It is therefore recommended that studies be undertaken to determine how much of the rapidly varying Doppler reflectivity and velocity fields can be regarded as turbulent fluctuations about a more slowly varying temporal mean or as actual rapid fluctuations. In other words, are the temporal changes in variables physically meaningful or are they simply random fluctuations or undersampled fluctuations (of even more rapidly varying phenomena such as very high-frequency buoyancy/gravity waves) superimposed on physically meaningful, more slowly varying variables, which can be tracked as coherent features on the 10-s scale? The preceding question needs to be answered separately for different phenomena and at different altitudes. For example, it is expected that tornadic supercells in the vicinity of the main updraft or the rear-flank downdraft have very rapidly varying variables and that rapid-scan observations should possess higher-amplitude temporal fluctuations than weaker convective systems, outside of any strong updrafts or downdrafts.

It is also recommended that experiments be undertaken to determine whether or not assimilating rapid-scan data into a numerical cloud model can improve the representation of nonmeasured (retrieved) variables or can improve short-term forecasts. Hu and Xue (2007) found that a high frequency of assimilating WSR-88D data does not necessarily lead to improvements, owing to "significant" adjustments during the initial forecast period. This issue needs to be explored further with rapid-scan data, especially after the initial forecast period. It is likely that there is no advantage to assimilating data on the time scale of the time step used in the model. However, it may be possible to assimilate the storm-scale data at short time intervals into large-eddy simulation (LES) models, so that the rapid-scan radar data can yield reasonable features on much smaller space (and time) scales.

In assimilating data into a cloud model and/or considering the evolution of a storm's structure, the maximum elevation angle must be considered. When a storm is relatively close, higher elevation angles must be scanned to probe middle and high levels in the storm. A decision must be made in the field whether to scan only to 20° elevation angle in STF-E mode or to repeat scans to 55°, with the tradeoff of increasing the volumetric scan time.

It may be possible to use the Tracking Radar Echoes by Correlation (TREC) technique (Rinehart 1979) with rapid-scan data. Kramar et al. (2005) used TREC to estimate the low-level wind field in a supercell using mobile Doppler radar reflectivity observations from the UMass X-Pol radar. It was noted how TREC fails to work when there is

strong vertical advection or updraft propagation. If the time between volume scans is decreased, then it is possible that these shortcomings may be lessened. By using TREC-based wind field estimates and fitting them variationally to the Doppler velocity field, it may be possible to obtain an improved analysis. Such a procedure is similar to that of those who have used variational techniques (adjoint methods) and a reflectivity-conservation equation (e.g., Qiu and Xu 1992). Since attenuation in the vicinity of heavy precipitation is serious enough to lead to extinction in some cases, the use of reflectivity tracking/ reflectivity conservation may be limited to portions of storms without extensive intervening heavy precipitation. Shapiro et al. (2003) found evidence that increased volumetric update frequency can improve the retrieval of the wind field from Doppler radar data using adjoint techniques.

While it may be revealing to pair the MWR-05XP with another rapid-scan radar such as the Rapid-DOW or the NWRT PAR in Norman, along a suitable baseline to collect rapid-scan, volumetric dual-Doppler data, it may not be practical to do so. Aside from issues of varying spatial resolution among all the radars, it would be very difficult, if not impossible, to scan a storm with the exact same volumetric update time; in other words, the difference in time between data collected by each radar at a point in space may be comparable to the volumetric update time. A possible solution might be to pair the MWR-05XP with an identical radar system.

Another issue that needs to be addressed is the time and effort spent on editing data (de-aliasing velocity folding, removal of second-trip echoes, etc.). Since the frequency of volumetric updates is much higher, an order of magnitude more data needs to be edited (e.g., the rapid-scan volumetric update time for a 60° sector up to 20° elevation angle is 7 s, while the equivalent volumetric update time for the UMass X-Pol is ~90 s). Thus, it becomes more important to devise even more efficient methods for dealiasing Doppler velocity data, etc.

One disadvantage of the MWR-05XP is that its beamwidth is relatively broad, so that the radar must be located very close to the target storm. In the future, it would be helpful if a narrower-beam antenna, around 1° could be obtained.

The MWR-05XP might be suitable for some clear-air boundary layer studies, but to increase its sensitivity, there would have to be some sacrifice in spatial and temporal resolution and/or maximum unambiguous range. Determining what the tradeoffs are quantitatively needs to be considered.

Postscript: The MWR-05XP was used in 2009 during year 1 of Verification of the Origins of Rotation in Tornadoes Experiment 2 (VORTEX2) which was conducted in the U. S Great Plains region (www.vortex2.org/). Its main role was rapidscan data collection on the storm scale. During VORTEX2, the MWR-05XP (with frequency hopping implemented to eliminate beam smearing in the STF-E mode) collected volumetric data every 6-7 s, within 10 km of a tornadic supercell, from 15 min before the birth of the tornado until after the tornado had dissipated. When the tornado was at maximum intensity, the radar was 5-6 km from the tornado. The MWR-05XP will be used again during year 2 of VORTEX2 in 2010. A pulsed, 2 μm-wavelength Doppler lidar was added to the radar platform during the summer of 2009 to allow close-range clear-air data collection to complement the radar data collection.

ACKNOWLEDGMENTS. Chad Baldi (ProSensing) led the data collection and field operations and Bethany Seeger (ProSensing) did much of the data processing. This work was supported in part by NSF Grant ATM-0637148 to the University of Oklahoma and contracts to ProSensing from the NAVY SBIR program at the Office of Naval

Research. Jeff Snyder (OU), Jana Houser (OU), and Mark Laufensweiler (OU) provided assistance in transferring data to our computer system; the former two also contributed to many of the missions. Paul Buczynski (NPS) also participated in the project. Curtis Alexander (NOAA/ Earth System Research Laboratory) provided some assistance with unfolding algorithms. Jim Mead (ProSensing) provided helpful comments on the initial draft of this manuscript. The first author is grateful to the Mesoscale Microscale Meteorology (MMM) Division at the National Center for Atmospheric Research (NCAR) for hosting his sabbatical visit in 2009.

Sidebar

A mobile X-band, phased-array Doppler radar was acquired from the U.S. Army by the Center for Interdisciplinary Remotely Piloted Aircraft Studies (CIRPAS) at the Naval Postgraduate School and adapted for meteorological use by ProSensing, Inc. The radar was used during field experiments conducted in the Southern Plains by faculty and students from the School of Meteorology at the University of Oklahoma during the spring storm seasons of 2007 and 2008. During these field experiments, storm-scale, rapid-scan, volumetric, Doppler-radar observations were obtained in tornadic and nontornadic supercells, quasilinear mesoscale convective systems, and in both boundary layer-based and elevated ordinary convective cells. A case is made for the use of the radar for studies of convective weather systems and other weather phenomena that evolve on time scales as short as tens of seconds. (Page 579)

References

REFERENCES

Biggerstaff, M. I., and Coauthors, 2005: The Shared Mobile Atmospheric Research and Teaching Radar: A collaboration to enhance research and teaching. *Bull. Amer. Meteor. Soc.*, 86, 1263-1274.

Bluestein, H. B., 1999: A history of severe-storm-intercept field programs. *Wea. Forecasting*, 14, 558-577.

_____, 2008: On the decay of supercells through a "downscale transition": Visual documentation. *Mon. Wea. Rev.*, 136, 4013-4028.

_____, 2009: The formation and early evolution of the Greensburg, Kansas, tornadic supercell on 4 May 2007. *Wea. Forecasting*, 24, 899-920.

_____, E. W. McCaul Jr., G. P. Byrd, and G. R. Woodall, 1988: Mobile sounding observations of a tornadic storm near the dryline: The Canadian, Texas, storm of 7 May 1986. *Mon. Wea. Rev.*, 116, 1790-1804.

_____, W.-C. Lee, M. Bell, C. C. Weiss, and A. L. Pazmany, 2003: Mobile Doppler radar observations of a tornado in a supercell near Bassett, Nebraska, on 5 June 1999. Part II: Tornado-vortex structure. *Mon. Wea. Rev.*, 131, 2968-2984.

_____, C. C. Weiss, M. M. French, E. M. Holthaus, R. L. Tanamachi, S. Frasier, and A. L. Pazmany, 2007a: The structure of tornadoes near Attica, Kansas, on 12 May 2004: High-resolution, mobile, Dopplerradar observations. *Mon. Wea. Rev.*, 135, 475-506.

- ____, M. M. French, R. L. Tanamachi, S. Frasier, K. Hardwick, F. Junyent, and A. L. Pazmany, 2007b: Close-range observations of tornadoes in supercells made with a dual-polarization, X-band, mobile Doppler radar. *Mon. Wea. Rev.*, 135, 1522-1543.
- Brown, J. M., and K. R. Knupp 1980: The Iowa cyclonicanticyclonic tornado pair and its parent thunderstorm. *Mon. Wea. Rev.*, 108, 1626-1646.
- Brown, R. A., and V. T. Wood, 1991: On the interpretation of single-Doppler velocity patterns within severe thunderstorms. *Wea. Forecasting*, 6, 32-48.
- Crura, T. D., and R. L. Alberty, 1993: The WSR-88D and the WSR-88D operational support facility. *Bull. Amer. Meteor. Soc.*, 74, 1669-1687.
- Fujita, T. T, 1981: Tornadoes and downbursts in the context of generalized planetary scales. *J. Atmos. Sci.*, 38, 1511-1534.
- Heinselman, P. L., D. L. Priegnitz, K. L. Manross, T. M. Smith, and R. W. Adams, 2008: Rapid sampling of severe storms by the National Weather Radar Testbed phased array radar. *Wea. Forecasting*, 23, 808-824.
- Houze, R. A., Jr., B. F. Smull, and P. Dodge, 1990: Mesoscale organization of springtime rainstorms in Oklahoma. *Mon. Wea. Rev.*, 118, 613-654.
- Hu, M., and M. Xue, 2007: Impact of configurations of rapid intermittent assimilation of WSR-88D radar data for the 8 May 2003 Oklahoma City tornadic thunderstorm case. *Mon. Wea. Rev.*, 135, 507-525.
- Kramar, M. R., H. B. Bluestein, A. L. Pazmany, and J. D. Tuttle, 2005: The "Owl Horn" radar signature in developing Southern Plains supercells. *Mon. Wea. Rev.*, 133, 2608-2634.
- Markowski, P. M., 2002: Hook echoes and rear-flank downdrafts: A review. *Mon. Wea. Rev.*, 130, 852-876.
- ____, Y. Richardson, E. Rasmussen, R. Davies-Jones, and R. J. Trapp, 2008: Vortex lines within low-level mesocyclones obtained from pseudo-dual-Doppler radar observations. *Mon. Wea. Rev.*, 136, 3513-3535.
- Pazmany, A. L., 2007: Electronically scanned radars for weather observations. Preprints, 33rd Conf. on Radar Meteorology, Cairns, Australia, Amer. Meteor. Soc, 7.1.
- Qiu, C-J., and Q. Xu, 1992: A simple adjoint method of wind analysis for single-Doppler data. *J. Atmos. Oceanic Technol.*, 9, 588-598.
- Rasmussen, E. N., and J. M. Straka, 1998: Variations in supercell morphology. Part I: Observations of the role of upper-level storm-relative flow. *Mon. Wea. Rev.*, 126, 2406-2421.
- ____, _____, M. S. Gilmore, and R. Davies-Jones, 2006: Preliminary survey of rear-flank descending reflectivity cores in supercell storms. *Wea. Forecasting*, 21, 923-938.

Rinehart, R. E., 1979: Internal storm motions from a single non-Doppler weather radar. NCAR Tech. Rep. NCAR/TN-146+STR, 262 pp.

Sandifer, J. B., 2005: Meteorological measurements with a MWR-05XP phased array radar. M. S. thesis, Naval Postgraduate School, Monterey, CA, 79 pp.

Shapiro, A., P. Robinson, J. Wurman, and J. Gao, 2003: Doppler velocity retrieval with rapid-scan radar data. *J. Atmos. Oceanic Technol.*, 20, 1758-1775.

Sirmans, D., and R. J. Doviak, 1973: Pulsed-Doppler velocity isotach displays of storm winds in real time. *J. Appl. Meteor.*, 12, 694-697.

Skolnik, M. L., 1990: Radar Handbook. McGraw-Hill, 1200 pp.

Tanamachi, R., H. B. Bluestein, W.-C. Lee, M. Bell, and A. Pazmany, 2007: Ground-based velocity track display (GBVTD) analysis of W-band radar data in a tornado near Stockton, Kansas, on 15 May 1999. *Mon. Wea. Rev.*, 135, 783-800.

Trapp, R. J., E. D. Mitchell, G. A. Tipton, D. W. Effertz, A. I. Watson, D. L. Andra Jr., and M. A. Magsig, 1999: Descending and nondescending tornadic vortex signatures detected by WSR-88Ds. *Wea. Forecasting*, 14, 625-639.

_____, S. A. Tessendorf, E. S. Godfrey, and H. E. Brooks, 2005: Tornadogenesis from squall lines and bow echoes. I. Climatological distribution. *Wea. Forecasting*, 20, 23-34.

Weisman M. L., 1993: The genesis of severe, long-lived bow echoes. *J. Atmos. Sci.*, 50, 645-670.

_____, and J. B. Klemp, 1984: The structure and classification of numerically simulated convective storms in directionally varying wind shears. *Mon. Wea. Rev.*, 112, 2479-2498.

_____, and C. A. Davis, 1998: Mechanisms for the generation of mesoscale vortices within quasi-linear convective systems. *J. Atmos. Sci.*, 55, 2603-2622.

Wurman, J., and S. Gill, 2000: Finescale radar observations of the Dimmitt, Texas (2 June 1995), tornado. *Mon. Wea. Rev.*, 128, 2135-2164.

Zirnic D. S., and Coauthors, 2007: Agile-beam phased array radar for weather observations. *Bull. Amer. Meteor. Soc.*, 88, 1753-1766.

AuthorAffiliation

AFFILIATIONS: Bluestein and French - School of

Meteorology. University of Oklahoma, Norman, Oklahoma;

PopStefanija - ProSensing. Inc., Amherst. Massachusetts; Bluth

and Knorr - Naval Postgraduate School, Monterey, California

CORRESPONDING AUTHOR: Dr. Howard B. Bluestein, School
of Meteorology, University of Oklahoma , 120 David L. Boren
Blvd., Suite 5900. Norman. OK 73072

E-mail; hblue@ou.edu

The abstract for this article can be found in this issue, following the tab/e of contents.

DOI:10.175/2009BAMS2914.1

In final form 28 August 2009

©2010 American Meteorological Society

Word count: **7910**

Copyright American Meteorological Society May 2010

More like this



Cited by (33)

Documents with shared references (1038)

Related items

Search with indexing terms


Subject

- Meteorology
- Storms
- Radar systems
- Independent sample
- Data processing


More...

Search


ebrary e-books

1.  Evaluation of the Multifunction Phased Array Radar Planning Process



-
2.  Weather Radar Technology Beyond Nexrad



-
3.  Strategic Guidance for the National Science Foundation's Support of the A...



[Ask a Librarian!](#)

[Need help? Try Ask a Librarian! M-F 0800-1600 PT.](#)



[Contact Us](#) [Terms and Conditions](#) [Accessibility](#) [Privacy Policy](#)

[Cookie Policy](#)

Copyright © 2016 ProQuest LLC.